Mechanical Systems and Signal Processing 56-57 (2015) 150–172

Contents lists available at ScienceDirect

Mechanical Systems and Signal Processing

journal homepage: www.elsevier.com/locate/ymssp

Accurate bearing remaining useful life prediction based on Weibull distribution and artificial neural network

Jaouher Ben Ali [a,b,*], Brigitte Chebel-Morello [b], Lotfi Saidi [a], Simon Malinowski [b], Farhat Fnaiech [a]

[a] University of Tunis, National Higher School of Engineers of Tunis, Laboratory of Signal Image and Energy Mastery (SIME), 5 Avenue Taha Hussein. P.O. Box 56, 1008 Tunis, Tunisia
[b] FEMTO-ST Institute, AS2M Department, UMR CNRS 6174-UFC/ENSMM/UTBM, 25000 Besançon, France

ARTICLE INFO

Article history:
Received 10 January 2014
Received in revised form
1 October 2014
Accepted 29 October 2014
Available online 15 November 2014

Keywords:
Prognostics and Health Management (PHM)
Remaining useful life (RUL)
Rolling element bearings (REBs)
SFAM
Weibull distribution (WD)

ABSTRACT

Accurate remaining useful life (RUL) prediction of critical assets is an important challenge in condition based maintenance to improve reliability and decrease machine's breakdown and maintenance's cost. Bearing is one of the most important components in industries which need to be monitored and the user should predict its RUL. The challenge of this study is to propose an original feature able to evaluate the health state of bearings and to estimate their RUL by Prognostics and Health Management (PHM) techniques.

In this paper, the proposed method is based on the data-driven prognostic approach. The combination of Simplified Fuzzy Adaptive Resonance Theory Map (SFAM) neural network and Weibull distribution (WD) is explored. WD is used just in the training phase to fit measurement and to avoid areas of fluctuation in the time domain. SFAM training process is based on fitted measurements at present and previous inspection time points as input. However, the SFAM testing process is based on real measurements at present and previous inspections. Thanks to the fuzzy learning process, SFAM has an important ability and a good performance to learn nonlinear time series. As output, seven classes are defined; healthy bearing and six states for bearing degradation. In order to find the optimal RUL prediction, a smoothing phase is proposed in this paper. Experimental results show that the proposed method can reliably predict the RUL of rolling element bearings (REBs) based on vibration signals. The proposed prediction approach can be applied to prognostic other various mechanical assets.

1. Introduction

Currently, traditional concepts of preventive and corrective maintenance are gradually submitted at new constraints of advanced required maintenance tasks. Many new advanced methods are very welcomed by the users in order to prevent degradation of their equipment. Hence, whatever the used method, it is important to anticipate the occurrence of defects in order to use protective actions. The main objective of this maintenance type is to ensure the dependability of industrial

* Corresponding author at: University of Tunis, National Higher School of Engineers of Tunis, Laboratory of Signal Image and Energy Mastery (SIME), 5 Avenue Taha Hussein. P.O. Box 56, 1008 Tunis, Tunisia. Tel.: +216 96568115/+216 52276629; fax: +21672486044.
E-mail address: benalijaouher@yahoo.fr (J. Ben Ali).

http://dx.doi.org/10.1016/j.ymssp.2014.10.014
0888-3270/

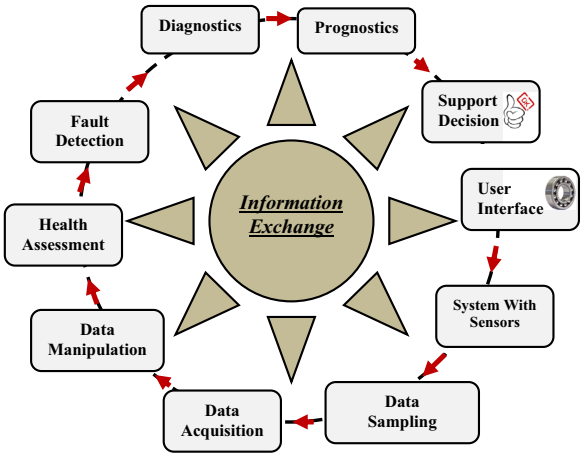

Fig. 1. PHM general scheme.

systems and to increase their availability with lower cost. The estimation of the remaining time of an equipment before failure helps the specialist in industries to avoid unnecessary spending time and money in maintenance. So, prognostics have become an important industrial issue and an appealing area of research to many researches. Prognostics are defined by the ISO 13381-1 as the estimation time to failure and risk of one or more existing assets and the prediction of future failure modes [1]. It is a promising activity that improves safety, availability of equipment and maintenance cost reduction. Prognostics and Health Management (PHM) is a process of detecting abnormal conditions, diagnosis of the fault and their cause and prognostics of the future fault progression [2].

In the literature, maintenance strategies are classified into three types [3]:

- Breakdown maintenance;
- Preventive maintenance;
- Condition-Based Maintenance (CBM).

Breakdown maintenance and preventive maintenance are disappearing from industrial practice as they are based on the repair of an asset when it breaks down, and periodic inspection and replacement. The main advantage of CBM is to control continuously a process to choose the best intervention time and to not interrupt normal operations. Thereby, CBM is widely targeted in research and industry nowadays. PHM, as shown in Fig. 1, is the most important activity of CBM. PHM is developed from fault detection to diagnostics and throughout prognostics. The main prognostic objective is to estimate the remaining time before total failure of assets [4]. So, reducing maintenance costs of critical industrial assets is one of the most important advantages of prognostics.

In the literature, there are three different approaches to prognostics [5]:

- The physical model developed by experts and validated on large sets;
- The rule based expert systems;
- The data-driven model.

In this work, we develop a novel data-driven prognostic approach based on vibration signals suitable for rotating mechanical assets. Our challenge is to define on a first hand a new feature which characterizes more accurately bearing degradations and on a second hand to simplify the prognostic task into a classification task. For this, we propose a new approach based on Weibull distribution and artificial neural network which is validated by an application on bearings. A modified Weibull Failure Rate Function (WFRF) called Universal Failure Rate Function (UFRF) is used to fit extracted features in the time domain based on vibration signals. Then, fitted features are used to train Simplified Fuzzy ARTMAP (SFAM) neural network. SFAM training mode is done with seven classes: healthy bearing and six states for bearing degradation. An intelligent smoothing phase is introduced to perform accurate RUL prediction. Experimental results based on bearing run-to-failure vibration signals demonstrate that the proposed method is able to track the regularity of bearing degradations sensitively and accurately.

The remainder of this paper is organized as follows: a detailed literature review is presented in Section 2 related to prognostics for bearing applications. Section 3 presents the different steps of the proposed method. In this section, the feature extraction process is given and the basic principles of Weibull distribution and SFAM neural network are detailed. Section 4 describes the simulation and experimental results as well as some numerical examples to assess the effectiveness of the proposed method. Section 5 is dedicated to discuss and analyse the experimental results by comparing the obtained performances with respect to other approaches. Finally, some conclusions and future works are provided in Section 6.

2. Motivation and related works

Rolling element bearings (REBs) are widely used in rotating machines. One of the fundamental problems currently faced a wide range of industries is how to identify a bearing fault before it reaches a critical level and even its catastrophic failure. REB is one of the important parts of rotating machinery and their failure is one of the most frequent reasons for machine breakdown. Approximately 45% of the failures are due to the bearing faults [6]. A failure survey by the Electric Power Research Institute (EPRI) indicates that bearing-related faults are about 40% among the most frequent faults in induction motors [7].

With the recent advances in modern technology, industry and scientist researchers are progressing toward providing expert systems to detect REB anomalies in an early stage and to predict, if possible, their remaining useful life (RUL).

Industrial systems are often very complex; it is very hard to build a formal model for prognostics. In [8], failure time values were first fitted to a Bernstein distribution to predict the RUL of bearings based on vibration signals. Despite the complexity of computation and the enormous simplification assumptions, the average prediction errors over all degradation percentiles were between 16.2% and 22.5%. In [9], single-point defects in REBs are modeled as a function (i) of the bearings' rotation of, (ii) of the load distribution, (iii) of the structure elasticity, (vi) of the oil film characteristics, and (v) of the transfer path between the bearing and the transducer. This work has focused only a particular case of bearing defects which is the single-point defect despite that a huge spreadsheet with several simplifications were used. We recall that bearing defects are classified into two classes; the single-point defects and generalized roughness [10]. As shown in Fig. 2, single-point defects are localized and classified into:

i. Outer race way defect;
ii. Inner race way defect;
iii. Ball defect.

Generalized roughness is a type of fault where the condition of a bearing surface has degraded considerably over a large area and become rough, irregular, or deformed. This type of defects is not considered in [9].

The most used technique in the literature is the data-driven approach due to the modeling complexity of industrial systems. Besides, the development and progression of sensors allow retrieving data on real time easily. Typically, two measures were often used for the diagnosis and the prognosis of bearings:

i. The stator current of Induction Machines (IMs) (if induction machines exist in the chain to prognosticate);
ii. The vibration signals.

Usually, if any fault occurred in IMs by means of one or more failed components, it will affect the behavior of the stator current [11]. However, several existing industrial applications do not rely on the use of IMs. For example, the health assessment of bearings in automobile engines cannot be followed using the stator current of IMs. In contrast to the stator current measurement, bearing vibration signals can be measured in all industrial systems. However, they are considered as non-stationary and nonlinear which present serious troubles in the study of this type of signals [12].

A lot of work about the REB prognosis based on vibration signals has been published. In several applications and benchmark studies, the Multi Layer feed-forward neural networks based on Multi-Valued Neurons (MLMVN) have demonstrated their ability to extract complex dynamic patterns from time series for mid-term and long-term predictions [13].

In [14], Feed Forward Neural Network (FFNN) with Levenberg Marquardt training algorithm is used to predict the RUL of bearings. One bearing was used in the training phase and in the test phase: the method cannot be generalized and we cannot judge its reliability by using the same bearing in the learning and test modes.

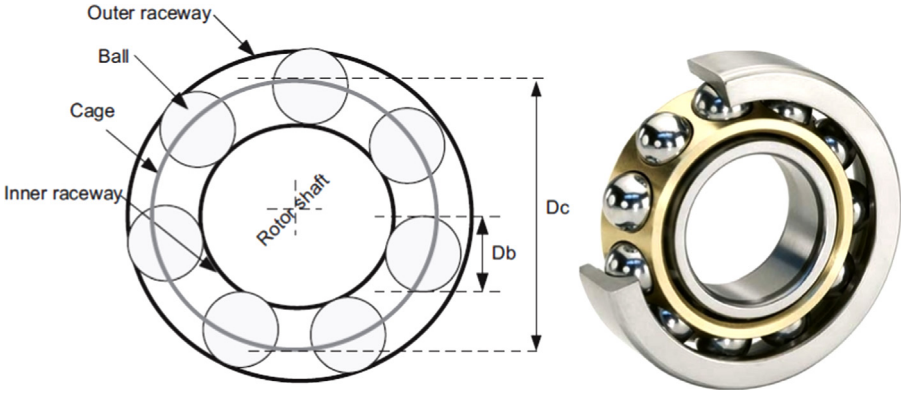

Fig. 2. Geometry of REB.

In [15], Weibull distribution and Artificial Neural Network (ANN) are used to predict the RUL of pump bearings. The error between estimated and actual RULs was high at the beginning of the experiment and it decreased just at the end of the experiment where the REB degradation symptoms become very important.

In [16], the Isometric feature Mapping reduction technique (ISOMAP) and Support Vector Regression (SVR) are used for prognostics of bearing fault degradations. Three bearings with different lifetimes were used to test the efficacy of the method. The major disadvantage of this technique is that the calculation of the RUL is performed by defining a failure threshold to the regression model where the choice of this threshold was intuitive and no scientific argument is given.

A challenge in bearing diagnosis and prognosis is to select the most sensitive parameters for the various types of fault, especially when the characteristics of failures are difficult to detect [17]. In the time domain, the selection of bearing assessment features is not sufficient, a fitted phase is necessary. Weibull distribution is a very powerful tool to represent various practical life time distributions. It is flexible enough to represent distributions with different scales and shapes [18]. In [14,15], Weibull hazard rate function is used to fit RMS and Kurtosis values to train an Artificial Neural Network (ANN) for bearing RUL prediction.

In this work, a new prognostic approach which can be applied on mechanical assets is proposed. This approach consists of three main steps as follow:

1. Feature extraction.
2. Classification task.
3. RUL estimation.

As strengths, in this work an effort is made to:

i. Define a new feature that follow bearing degradation more accurately than classical statistical time domain features;
ii. Convert the prognostic task into a classification task;
iii. Transform classification results into an accurate RUL prediction.

The diverse steps of the proposed method are detailed in the next section.

3. Description of the proposed approach

The new proposed method has the goal to achieve more accurately bearing RUL prediction. As shown in Fig. 3, two major steps are proposed:

- The offline step: In this step, one full bearing run-to-failure history is used to select the optimum SFAM structure. Also, to ensure stability to the created SFAM, the Weibull distribution (WD) is used to fit features before using them as input to the SFAM.
- The online step: Unlike the first step, features are extracted online each ten minutes from new bearing (not used in the offline step). The time and the type of failure of this bearing are unknown. The extracted features are used without fitting as input of the SFAM neural network. Thereby, the class of these features is estimated and consequently the degradation

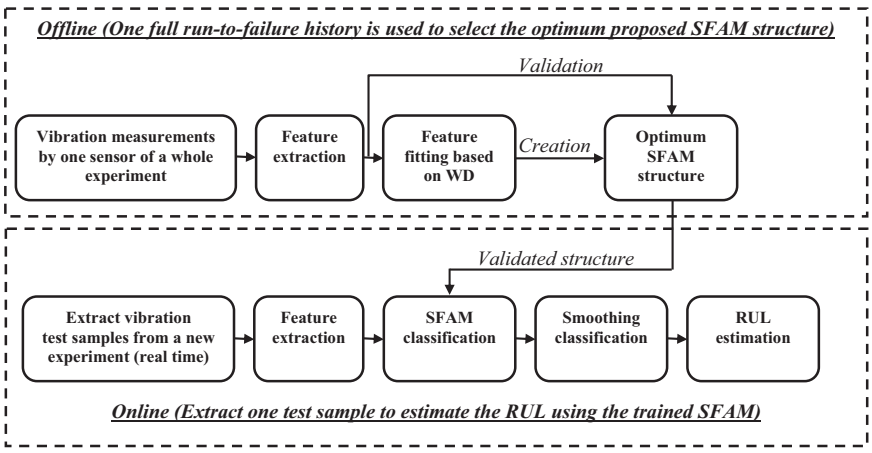

Fig. 3. Proposed framework to estimate bearing RUL.

Table 1
RMS and Kurtosis expressions.

Root mean square (RMS)	$\left(\frac{1}{N}\sum_{i=1}^{N} x_i^2\right)^{1/2}$
Kurtosis	$\frac{1}{N}\sum_{i=1}^{N} \frac{(x_i-\bar{x})^4}{\sigma^4}$

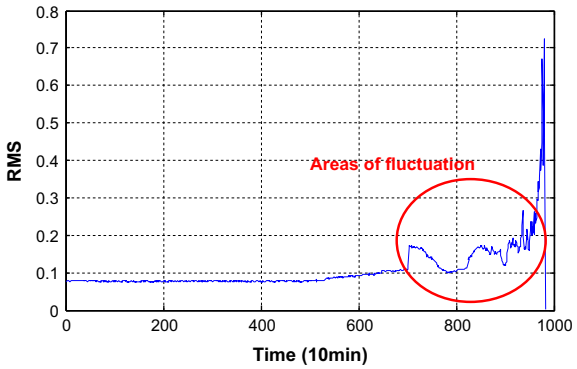

Fig. 4. RMS measurement.

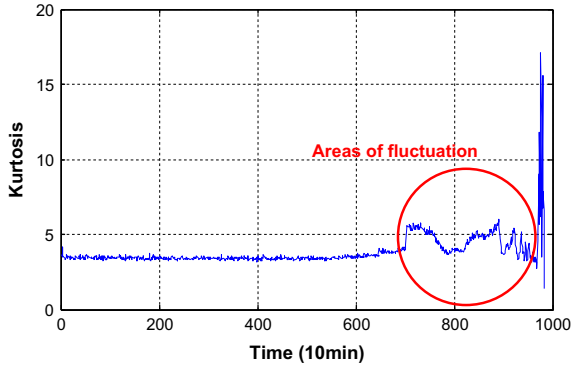

Fig. 5. Kurtosis measurement.

rate is given. However, classification results of the proposed SFAM cannot be directly used as an accurate prediction of the RUL. Hence, a new smoothing algorithm based on two successive SFAM classifications is proposed.

A detailed description of the proposed methodology is given as follow.

3.1. *Feature extraction*

In the literature, the most used features for the diagnosis and prognosis of bearings are the RMS and the Kurtosis defined respectively in Table 1 [14,15,19].

Real examples of RMS and Kurtosis measurements extracted from a run-to-failure history of the same bearing are respectively shown in Figs. 4 and 5. The evolution of RMS and Kurtosis curves show several areas of fluctuation which raises problems for the prognostic task.

The areas of fluctuation are due to several factors. Firstly, each rolling element has a different effective rolling diameter and is tried to roll at a different speed, but the cage limits the deviation of the rolling elements from their mean position, thus causing some random slip [6]. Secondly, noises degrade the measurement quality and generally they are greater than the amplitude of the first low anomalies. Moreover, the relatively weak bearing signals are always affected by quite stronger signals (gears, bars,…). All these cause areas of fluctuation for bearing features in the time domain.

To avoid these fluctuations and to improve the quality of the proposed prognostic approach, we propose a new measurement to monitor bearing degradations. The proposed measurement is the RMS Entropy Estimator (RMSEE) which is

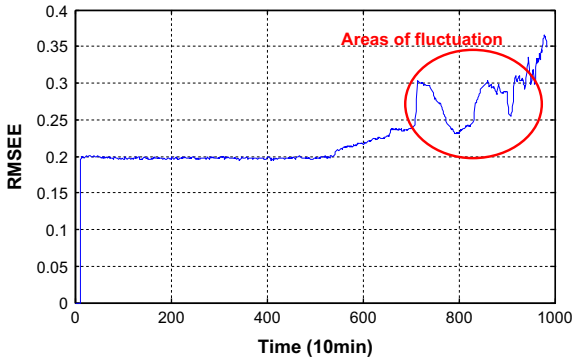

Fig. 6. RMSEE measurement.

computed as:

$$\mathrm{RMSEE}(i) = \frac{1}{n}\sum_{i=1}^{n} -\mathrm{RMS}(i)\log(\mathrm{RMS}(i)), \tag{1}$$

where ($n=10$) is the sliding window length.

The following steps summarize the implementation of the RMSEE:

- Set the RMSEE to zero;
- Select a sliding window (sliding step = 1, window length = 10) to browse all points of the RMS measurement;
- For each point of the window, calculate the RMSEE (Eq. (1));
- After 10 sliding steps, calculate the average RMSEE and maintain this value;
- Increment the sliding window with one sliding step and recalculate the RMSEE for the next 10 RMS points;

Fig. 6 shows the RMSEE measurement of the same bearing used to compute the previous RMS and Kurtosis features. Compared to the RMS and Kurtosis measurements, the RMSEE exhibits fewer fluctuations, which can improve the classification task. Moreover, RMS and kurtosis values come down and decrease when the damage is well advanced [20] unlike the proposed RMSEE feature.

The first nine points of the RMSEE are equal to zero due to the sliding window length which set to ten. Despite the fact that increasing window length decreases fluctuations, it increases the number of zero points and the computational time. Theoretically, the magnitude of time domain features should increase when bearing degradations become more severe. This type of degradation is well known in the literature as ideal degradation where the evolution of time domain features is mainly monotonically increasing and represents an ideal case [21]. However, sudden degradation is the most existing type of bearing defects in industrial environments. In most cases, the degradation appears suddenly and does not depict a slow monotonic behaviour [21]. Thereby, it is not obvious to use only classical time domain features. In this fact, we have proposed the RMSEE feature which can follow bearing degradation more accurately than classical time domain statistics. However, the computation of the RMSEE is based on a moving window where the choice of the window length should be done precisely. Consequently, 50 tests have been performed in this work to select the most effective length of the RMSEE window. The window length is varied from 2 to 50 and for each case the RMSEE monotonicity is then evaluated. The evaluation of monotonicity M was proposed in [4] and it is computed as follow.

$$M = \left| \frac{\text{number of } d/dx > 0}{n-1} - \frac{\text{number of } d/dx < 0}{n-1} \right| \tag{2}$$

where n is the number of observations in the evaluated feature and d/dx is the differentiation operator, which becomes the difference between two successive points for discrete signals. Monotonicity M is measured by absolute difference of positive and negative derivatives. The value of M can be from 0 to 1: highly monotonic features will have $M=1$ and non-monotonic features $M=0$. By evaluating the monotonicity of the proposed RMSEE, the best window length is chosen. The best window length ensures to the RMSEE more credibility in terms of monotonicity and elimination of areas of fluctuation. As a result, 10 points are used to compute the RMSEE in each window.

In this section, three features are computed and selected: the RMS, the Kurtosis and the RMSEE. Then, the Weibull distribution is adopted to fit these features and to guarantee more. In the next sub-section, we will present the process of feature fitting.

Table 2
The Weibull distribution.

Probability density function	$f(t,\beta,\eta,\gamma)=\frac{\beta}{\eta}\left(\frac{t-\gamma}{\eta}\right)^{\beta-1}\exp\left(-\left(\frac{t-\gamma}{\eta}\right)^{\beta}\right)$
Cumulative distribution function	$F(t,\beta,\eta,\gamma)=1-\exp\left(-\left(\frac{t-\gamma}{\eta}\right)^{\beta}\right)$
Reliability function	$R(t,\beta,\eta,\gamma)=\exp\left(-\left(\frac{t-\gamma}{\eta}\right)^{\beta}\right)$
Failure rate function	$\lambda(t,\beta,\eta,\gamma)=\frac{\beta}{\eta}\left(\frac{t-\gamma}{\eta}\right)^{\beta-1}$

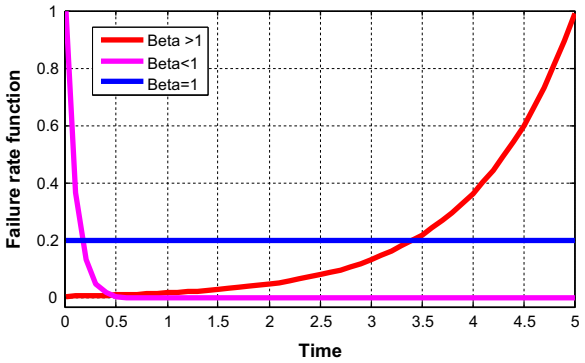

Fig. 7. The shape parameter influence on the failure rate function.

Table 3
Estimated UFRF parameters.

	η	β	Y	K
RMS	281.0209	12.0917	0.0773	1.38×10^{-5}
Kurtosis	86.7537	11.8280	3.4471	3.8×10^{-10}
RMSEE	100	5	1.9796	3.55×10^{-4}

3.2. Feature fitting based on Weibull distribution

Inspired from his name, "Waloddi Weibull" in 1936 has discovered his famous probability distribution called Weibull Distribution (WD) [22]. The WD can preferably reflect the fatigue strength and fatigue life of mechanical products and their parts under random loads [23]. WD is defined in Table 2 by three parameters: $\beta>0$ is the shape parameter, $\eta>0$ is the scale parameter and $\gamma>0$ is the position parameter. The stochastic variable with the same scale η unit is $t>\gamma$. The model is reduced to the common two parameters by setting $\gamma=0$. The influence of the shape parameter on the failure rate function is shown in Fig. 7.

WD is extremely important to characterize probabilistic behaviors of a large number of real phenomena. This distribution is especially used as a failure model to analyze the reliability and maintainability of different system types [24]. This paper presents a modified Weibull Failure Rate Function (WFRF) called Universal Failure Rate Function (UFRF) for bearing feature fitting in the time domain. The proposed UFRF is defined as:

$$\lambda(t,\beta,\eta,Y,K)=Y+K\frac{\beta}{\eta^{\beta}}t^{\beta-1}, \tag{3}$$

where $\beta>0$ is the shape parameter and $\eta>0$ is the scale parameter. The parameter K is introduced to scale the fitted measurement values to any ranges, and the parameter Y is introduced to indicate the value when the time is 0. Table 3 shows the estimated parameters to fit RMS, Kurtosis and RMSEE features.

To evaluate the importance of the estimated UFRF parameters, Figs. 8–10 show respectively the fitting of the extracted RMS, Kurtosis and RMSEE measurement. The three fitted measurements show no areas of fluctuation which is very interesting to be used to train the expert system and to predict the RUL of bearings.

Fitting features is a necessary step to produce monotonic features that better characterize the degradation phenomenon over time. This assumption is not valid for some components such as batteries, which may have a certain degree of self repair for short periods of non-use. However, for mechanical components and for systems with a combination of electronic and mechanical components, this assumption holds [4]. This argument justifies our use of a fitting phase for bearing features before using the neural classifier.

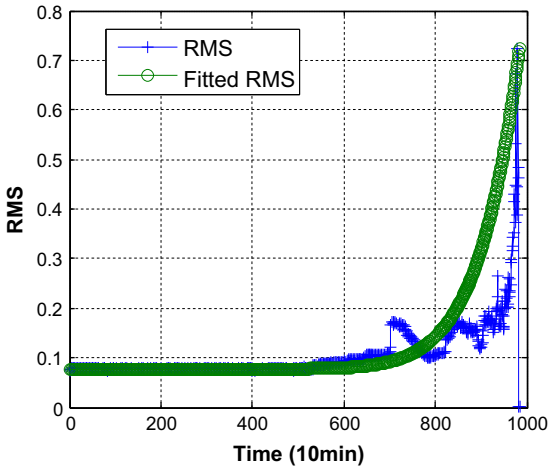

Fig. 8. Fitted RMS measurement.

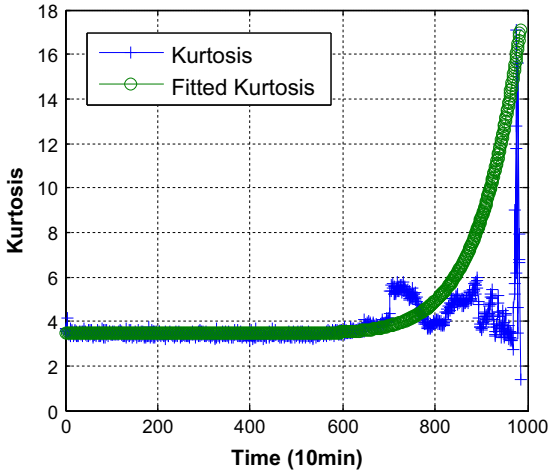

Fig. 9. Fitted Kurtosis measurement.

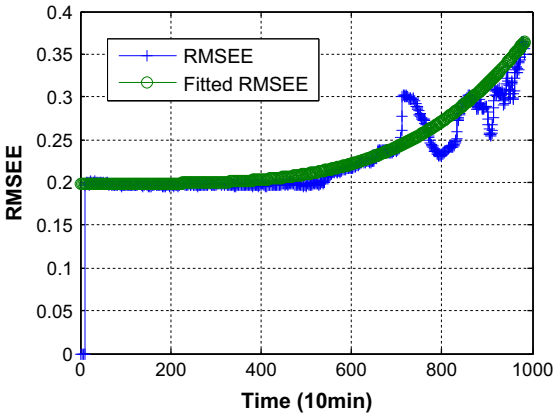

Fig. 10. Fitted RMSEE measurement.

In this paper, three features are selected and fitted using the WD. We recall that feature fitting is only used in the offline mode to select the optimum SFAM structure. However, in online mode (SFAM test mode), the three extract features should be used directly as SFAM inputs without fitting. So, the use of Weibull distribution is just employed to create the SFAM classifier. In the next section, the different steps of SFAM algorithm are given.

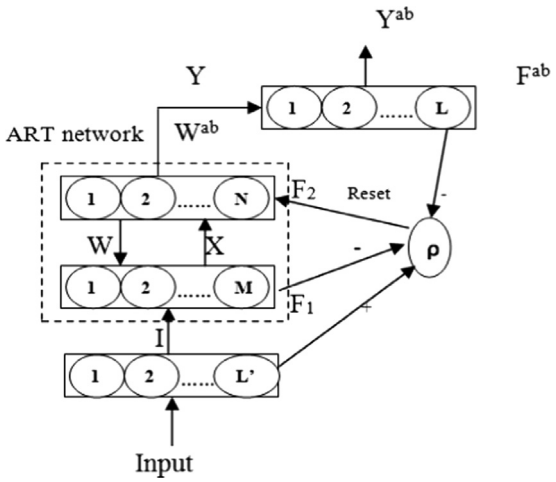

Fig. 11. SFAM neural network architecture.

3.3. The simplified Fuzzy adaptive resonance theory map neural network (SFAM)

After fitting the selected features, it is required to combine them with a neural network classifier to predict the RUL. Hence, this section is devoted to present the different steps of the used neural network classifier.

The Fuzzy ARTMAP is a neural network introduced by Carpenter, Grossberg and Rosen in 1991 [25], which is a modified version of the binary ART [26]. This network may accept analog fuzzy input patterns, i.e. vectors with component values between 0 and 1. The Fuzzy ARTMAP is a supervised neural network able to perform incremental learning, i.e. it can learn continuously without forgetting what it has previously learned. The Simplified Fuzzy ARTMAP (SFAM) neural network is a fast incremental supervised learning system for analog inputs. In 1993, Kasuba proposed the SFAM network which is a simplification of Fuzzy ARTMAP [27].This network is a step ahead of Fuzzy ARTMAP in reducing the computational and architectural size redundancy of Fuzzy ARTMAP [27]. Thus, the current study is based on the potential use of SFAM network for the classification process. The SFAM network has a simplified architecture when compared to the original Fuzzy ARTMAP [28].

As illustrated in Fig. 11, the SFAM is formed by three layers; the input layer F_1, the competitive layer F_2 and the output layer F^{ab}.

The activity patterns of layers F_1 and F_2 are fully interconnected. Each neuron is initially connected to every neuron on the other layer. All connections are weighted by synaptic weights lying between 0 and 1. Each neuron of the F_2 layer represents one category formed by the network and it is characterized by its weight vector W_j (j is the index of the neuron). The weight vector's size is equal to the dimension M of layer F_1. In the training process, if the weights of a neuron are not modified, this neuron is said uncommitted. On the other side, if a neuron's weights have been modified, this neuron is said committed.

SFAM is based on a form of normalization called complement coding. The operation consists on taking the input vector and concatenating it with its complement. The resulting vector should be presented to the layer F_1. Therefore, the dimension M of layer F_1 is double the input vector's dimension ($M=2L'$).

The F^{ab} layer is connected with the competitive layer F_2 by the W^{ab} weights to locate the appropriate class t of the input vector in the test mode. More details are given in the appendices.

For bearing degradation assessment, the SFAM neural network is used as follow:

- SFAM inputs: The input data used to train the SFAM are the three selected features. Each feature is fitted with the proposed UFRF function. Then, two points of each feature are used to train the classifier: the inspected point and the previous point. In this way, the size of input SFAM vector is equal to six and the training will be done $ft-1$ times where ft is the time of bearing failure.
- SFAM outputs: As outputs, L classes are proposed where the first class indicates the healthy bearing state and the other $L-1$ classes indicate the evolution of degradation rate. Fig. 12 shows an example of SFAM outputs where $L=7$ and this structure can be summarized as shown in Fig. 13. We should note that L is fined empirically by using several experiments.
- SFAM training mode: The fitted features based on WD of the first bearing are used as inputs and the predefined seven classes are used as the desired outputs.
- SFAM testing mode: The same features extracted from the same bearing are used without fitting to validate the trained SFAM. Thereby, the classification task will be done $ft-1$ times. Then, thanks to the SFAM classification, a class representing the bearing degradation rate is given for each input vector. Consequently, an estimation of the RUL will be made. After validation, the SFAM testing mode can be used online to estimate the RUL of other bearings which have not been used previously.

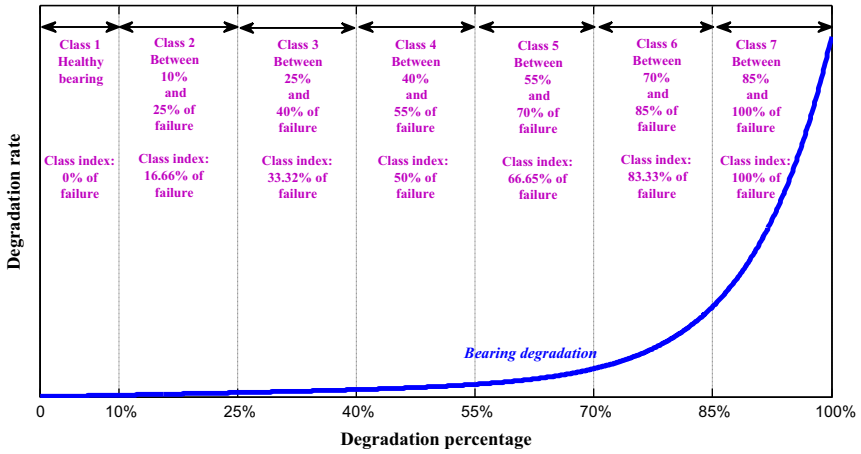

Fig. 12. Selection of SFAM outputs.

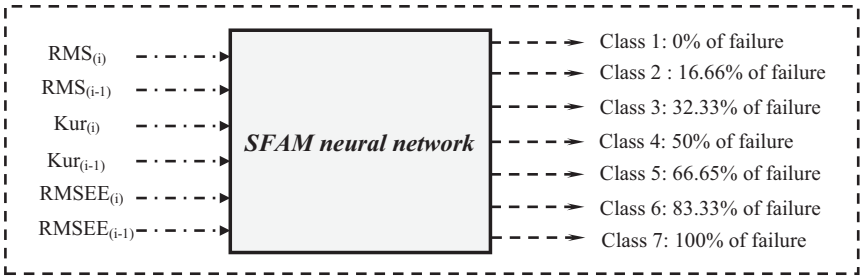

Fig. 13. Proposed SFAM structure.

Table 4
Smoothing prediction algorithm.

Initialization
Fix the number of smoothing iterations *si*
Set the start smoothing time *sst*
Repeat
Initialize the smoothing step $ss=0$
Repeat
Compute the smoothed RUL by
$\mathrm{RUL}(sts)=\frac{(RUL(sts)+RUL(sts-1))}{2}$
Increment the smoothing by
$ss=ss+1$
Until (*ss*=*si*)
Select the next point to inspect it
Until (the end of the experiment)

3.4. RUL estimation

As mentioned above, the classification results cannot be directly used as a bearing RUL prediction. So, another technique is required exploiting the RUL of the SFAM classes. In this section we propose a new smoothing algorithm where the classes are smoothed to follow more accurately the real bearing degradation. The main objective of the proposed smoothing algorithm is to compute the average of each two successive classes. The average process should be done $L-1$ times to find better smoothing results where L is the number of classes. The idea of choosing $L-1$ times of averaging inspired by the number of classes without taking into account the class of the healthy bearing state.

Table 4 summarizes the different steps of the proposed algorithm and experimental results based on this algorithm are given in the next section.

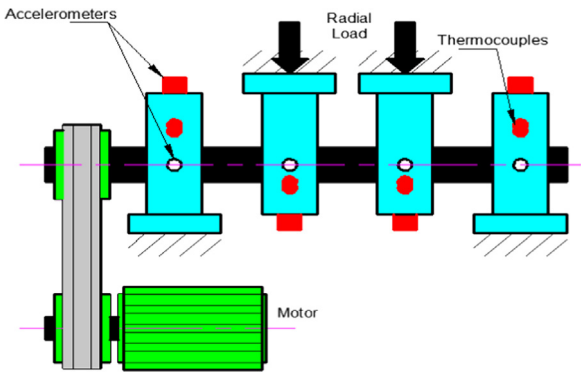

Fig. 14. Bearing test rig.

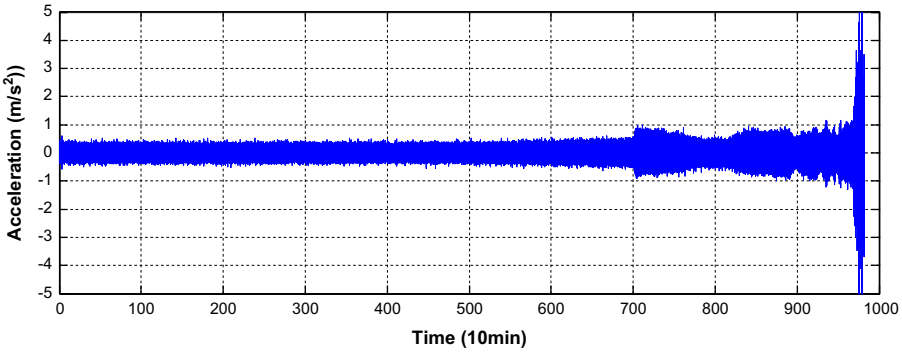

Fig. 15. Bearing 1 of testing 2 run-to-failure vibration signals ending with an outer race defect.

4. Experimental results

4.1. Experimental setup and data recording

Rexnord ZA-2115 double row bearings are installed on the shaft of the test rig. Bearings contain 16 rollers in each row, a pitch diameter of 2.815 in., a roller diameter of 0.331 in., and a tapered contact angle of 15.17° [29,30]. PCB 353B33 High Sensitivity Quartz ICP accelerometers are installed on the bearing housing. Sensor placement and test rig are shown in Fig. 14. All failures occurred after exceeding designed life time of the bearing which is more than 100 million revolutions.

Four bearings are installed on the shaft. The rotation speed is kept constant at 2000 rpm by an AC motor coupled to the shaft via rubber belts. A radial load of 6000 lbs is applied onto the shaft and bearing by a spring mechanism. All bearings are force lubricated.

The test is carried out for 35 days until a significant amount of metal debris is found on the magnetic plug of the test bearing [31]. In this way, it is possible to build bearing run-to-failure data sets with known defects.

Each data set describes a run-to-failure experiment. It consists of individual files that are 1-s vibration signal snapshots recorded at specific intervals (every 10 min). Each file consists of 20480 points with the sampling rate set at 20 kHz. Records (row) in the data file are data points.

Three tests (i.e., tests 1, 2, and 3; with each setup testing four bearings) are implemented in this experiment. Only bearing 1 of testing 2, bearing 3 of testing 1 and bearing 4 of testing 1 are used in this paper because they are the only ones that failed during the experiment. For more detailed information about this experiment, interested readers shall refer to [29–31]. Fig. 15 shows the bearing 1 of testing 2 run-to-failure vibration signals ending with an outer race defect. Fig. 16 shows pictures of bearing components after test (pictures from [31]) and Table 5 summarizes information of the three bearings studied in this work. The extracted RMS, Kurtosis and RMSEE features from the bearing 1 of testing 2 are shown respectively in Figs. 4–6.

Table 5 shows that the bearing life is highly nonlinear. Firstly, in spite of the use of 12 bearings in the three tests, only 3 failed. Secondly, despite the fact that the 3 failed bearings were of the same type and were used under the same conditions of speed and load, the type and time of breakage are not the same for these 3 bearings. Thirdly, the relatively weak bearing signals are always affected by quite stronger signals (gears, bars…). All these lead us to converge to a single question: What is the most effective method for bearing fault prognostics?

In the next section we present the experimental results of the proposed methodology which is very promising for prognostic activities.

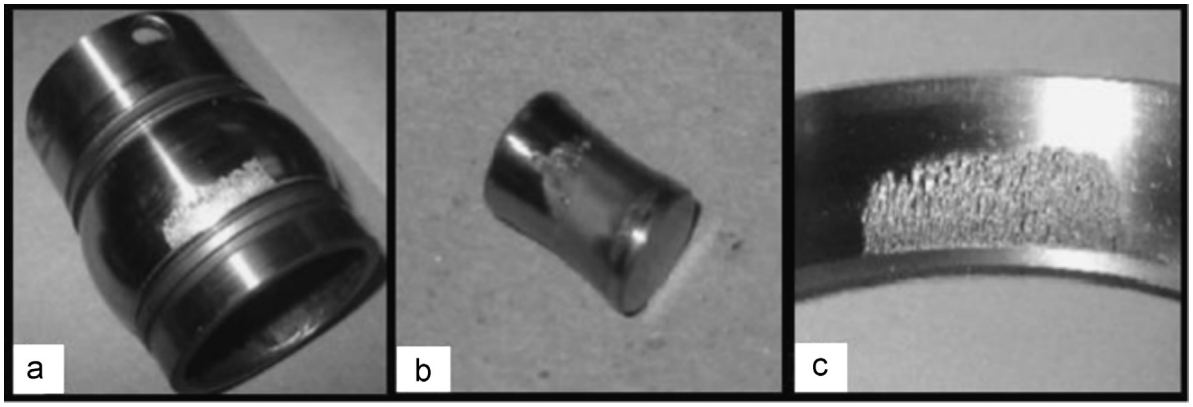

Fig. 16. Pictures of bearing components after test: (a) inner race defect, (b) roller element defect (c) outer race defect [31].

Table 5
Tested bearings information.

Bearing	Bearing type	Load (lbs)	Speed (rpm)	Type of degradation	Break time (10 min)	Maximum magnitude [m/s^2]
Bearing 1 of testing 2	Rexnord ZA-2115	6000	2000	Outer race	984	5
Bearing 3 of testing 1	Rexnord ZA-2115	6000	2000	Inner race	2155	5
Bearing 4 of testing 1	Rexnord ZA-2115	6000	2000	Roller	2155	4

4.2. Application of the proposed approach: Case study for bearing prognostics

SFAM inputs are the fitted RMS, Kurtosis and RMSEE values in the inspected time and previous time. Thereby, the size of any input vector I is $L'=6$ and I is defined as:

$$I=(RMS_{(i)}, RMS_{(i-1)}, Kurtosis_{(i)}, Kurtosis_{(i-1)}, RMSEE_{(i)}, RMSEE_{(i-1)}), \quad (4)$$

where i and $i-1$ are the time value at the current inspection point and the previous inspection point respectively.

This input structure has recently been used in several previous works. In [14,15,32], the age values (time) at the current and previous points with RMS and Kurtosis values are used as inputs for a feed forward neural network. In the proposed method, we planned using the RMSEE instead of the use of time. This change is considered because:

- SFAM inputs must be between 0 and 1. To meet this condition, we should know the maximum and minimum values for each feature. So, if we use the time as an input, we should know the final failure time that is already the objective of our study.
- To find monotonic features with minimal fluctuations remains a challenge for scientific researchers. In this sense, the proposed RMSEE has better specifications that features recently used in the literature (RMS and kurtosis).

As SFAM outputs, seven classes are used in the learning process describing the bearing degradation states ($L=7$).

First, the fitted RMS, Kurtosis and RMSEE using Weibull Distribution (WD) of bearing 1 of testing 2 are used to train the SFAM neural network. Then, the same features are used in real time, without WD fitting and point by point to evaluate the proposed SFAM skills. In this way, the SFAM neural network can be used to test other bearings which are not used previously in the training mode. So, thanks to the proposed methodology, one run-to-failure history is necessary to train the neural network and this is another advantage of the proposed method.

By applying the SFAM algorithm to the non fitted features of bearing 1 of testing 2, the neural network was able to identify all training data sets and the overall average classification accuracy (CA=74.2%) is achieved. The real measurements shown in Figs. 4–6 are used in the test phase. Although the huge zones of fluctuation in the not fitted features and despite the fact that training features and testing features are not the same (training with WD fitted features and testing with original features), classification results are acceptable. Table 6 summarises the classification accuracy for each class and Fig. 17 shows a good classification which follows the real bearing degradation.

For better accuracy, the smoothing algorithm is integrated for each two successive classification results. The smoothing mainly consists of an average, si times, of two successive classifications. This smart step makes the estimate of the RUL more continuous to follow more accurately the actual degradation of bearings. Experiment results shown in Fig. 18 confirm that better performance is achieved in order to predict bearing failure when we chose six smoothing iterations ($si=6$). Five and seven smoothing iterations, shown respectively by the green and the pink color, have more errors in terms of monitoring the RUL.

Table 6
Classes classification accuracies.

# of Class	0	1	2	3	4	5	6
# of vectors	393	98	99	98	99	98	99
# of well classified	392	95	68	57	43	62	14
CA (%)	99.75	96.93	68.68	58.16	43.43	63.26	14.14

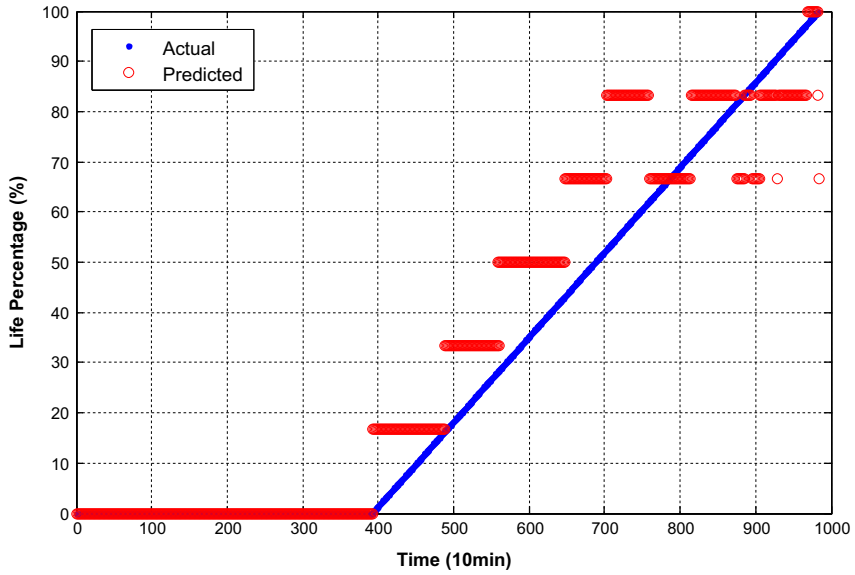

Fig. 17. Online classification of bearing rate failure.

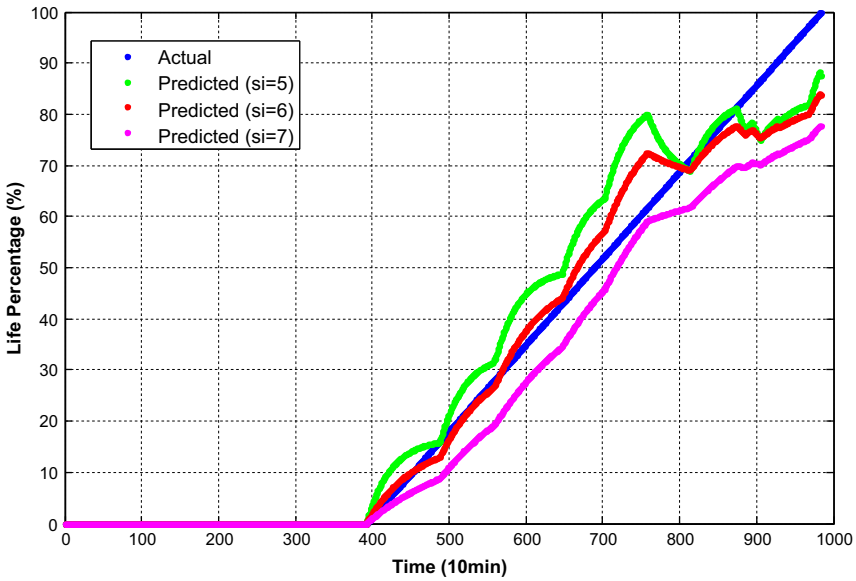

Fig. 18. Prediction results of the test failure history.

Fig. 18 shows the importance of SFAM for solving online classification problems. The bearing will totally fail after it reaches 984 units of time. The choice of six smoothing iterations is due to the number of classes already selected for classification regardless of the healthy bearing condition. Each class presents a degradation index of 16.66% compared to the previous class. As shown in Fig. 12, the seventh class shows 100% of the bearing life (total bearing failure).

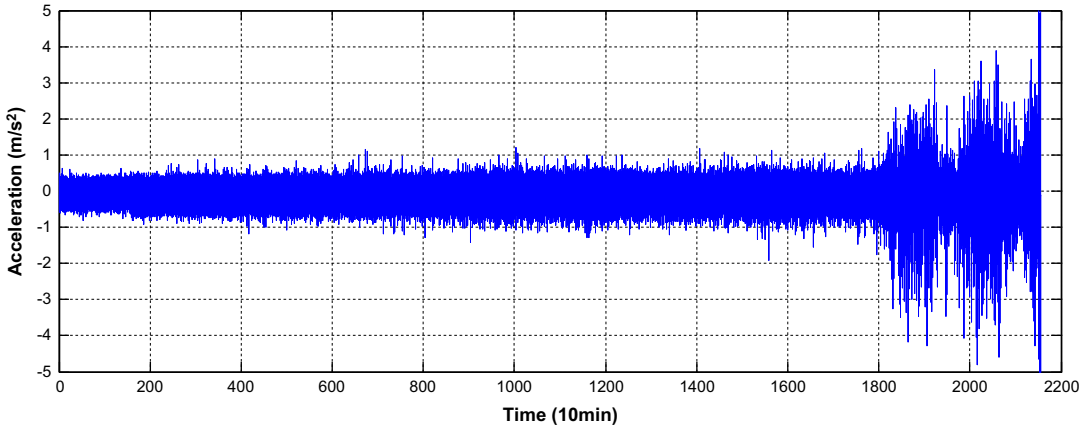

Fig. 19. Bearing 3 of testing 1 run-to-failure acceleration vibration signals ending with an inner race defect.

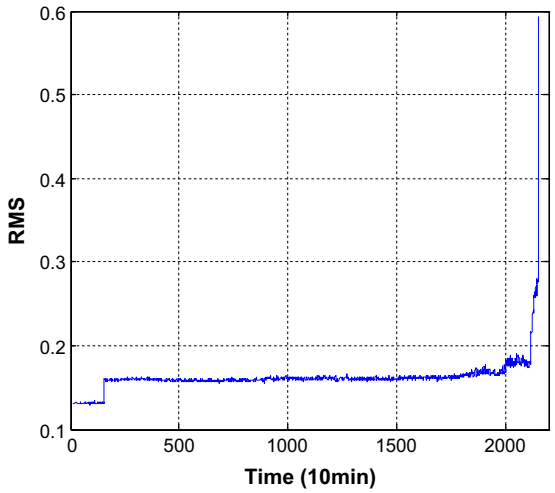

Fig. 20. RMS of the bearing 3 of testing 1.

The start time of the smoothing algorithm (*sst*) shown in Table 4 should be set to 11 because the calculation of the RMSEE begins after the first 10 measures of the experiment. Besides, we need two successive classification results to start smoothing.

The most faithful predicted RUL, shown by the red color in Fig. 18, can be used to estimate the remaining life of the tested REB. For example, when the current age is 650 days, the predicted RUL is 45.2%. The predicted failure time would be (650-393)/45.2%=569 (unit of time), and the RUL would be (569+393)−650=312 (unit of time). Consequently, it is easy to conclude that the estimated failure age is 650+312=962 (unit of time). The error between the theoretical and practical results is (984-962) × 100/984=2.23%.

The smoothing algorithm degrades at the end of the experiment, e.g., at the inspection point 964, the estimated life percentage is 80.04% and the real life percentage is 96.61%. This degradation does not influence the importance of the method. The most important for the industrial prediction tasks is to have estimations close to the actual values throughout the experiment and especially at its beginning.

Finally, we have revealed that the credibility of experimental results can be quantified by prognostic performance indicators to ensure that the predicted estimates can be considered trustworthy for decision-making in predictive maintenance activities.

For further evaluation, run-to-failure acceleration vibration signals of bearing 3 of testing 1 are used. This test contains 2155 records ever used in the SFAM training phase. Fig. 19 shows the bearing 3 of testing 1 run-to-failure acceleration vibration signals ending with an inner race defect. Figs. 20–22 show respectively the RMS, the Kurtosis and the RMSEE measurement of the tested bearing. These features are used as inputs for the trained SFAM network. So, without using the Weibull distribution for fitting, the state of the bearing degradation can be given for each measure thanks to the SFAM neural network. Consequently, by applying the proposed smoothing algorithm every two successive classification results, the RUL prediction can be done accurately. Prognosis results shown in Figs. 23 and 24 confirm the robustness of the proposed method. In addition, an encouraging interpretation is concluded; despite that the tested bearing has an unknown

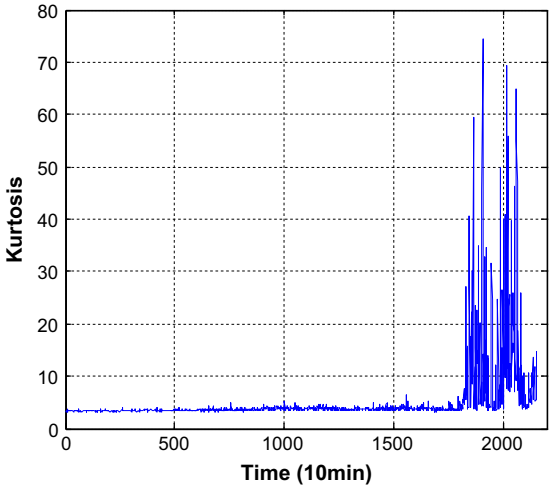

Fig. 21. Kurtosis of the bearing 3 of testing 1.

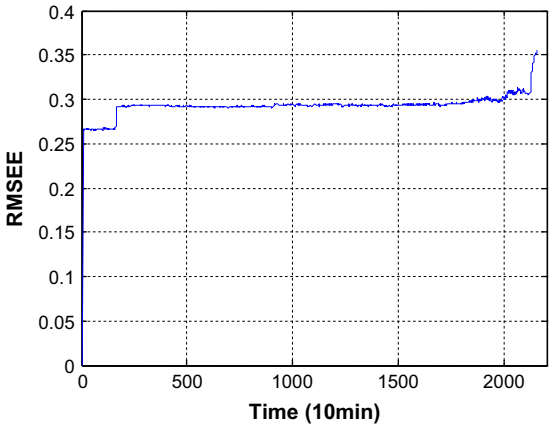

Fig. 22. RMSEE of the bearing 3 of testing 1.

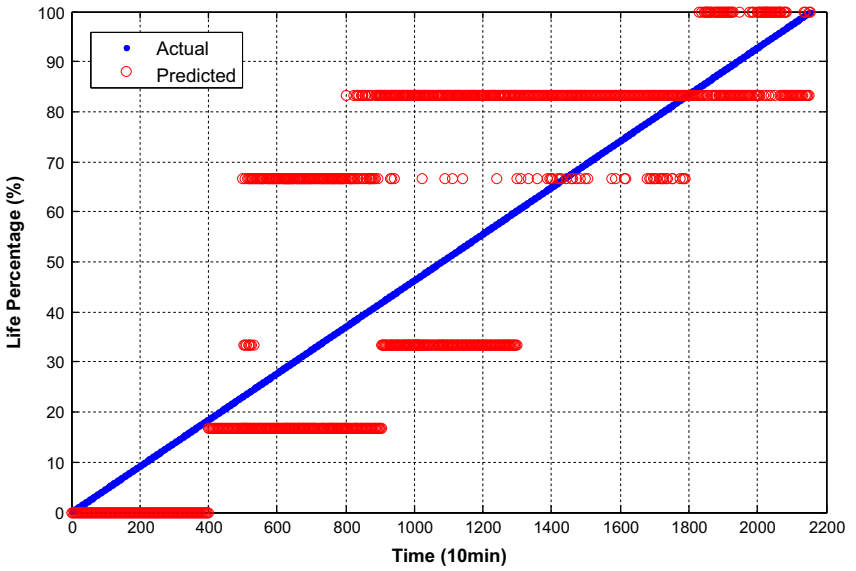

Fig. 23. Online classification of bearing rate failure (bearing 3 of testing 1).

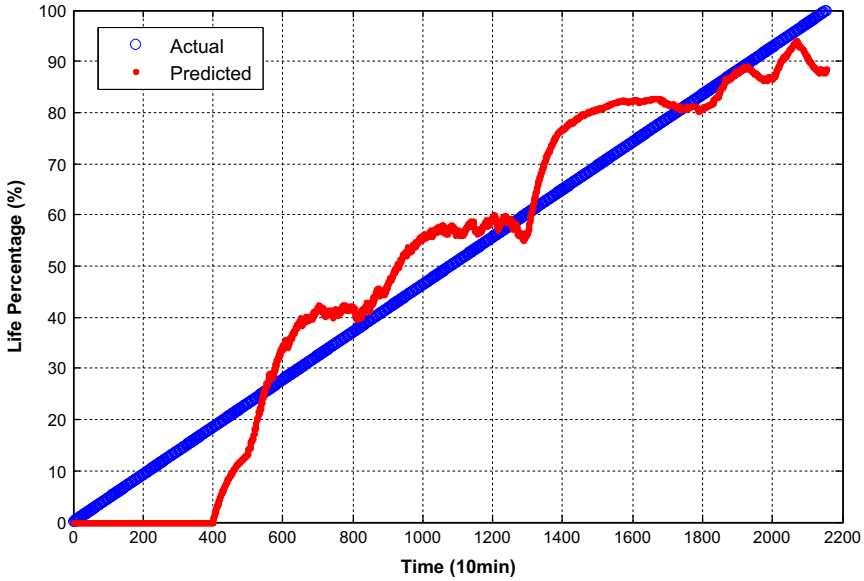

Fig. 24. RUL prediction of the bearing 3 of testing 1 test failure history.

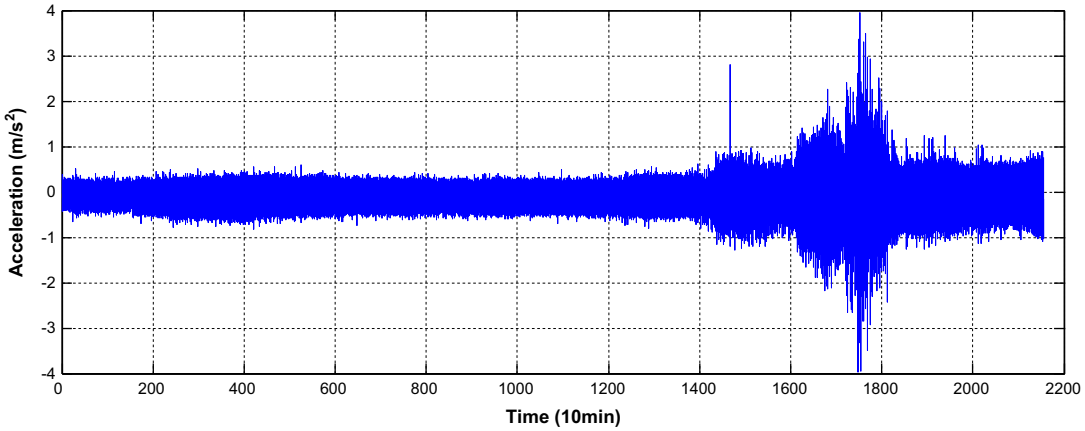

Fig. 25. Bearing 4 of testing 1 run-to-failure acceleration vibration signals ending with a roller. element defect.

defect for the SFAM, the neural network was able to estimate the RUL with substantial fidelity. Besides, the misclassifications shown in Fig. 23 are not very far from the real class, e.g., if the real class is 5 the predicted class is 4, 5 or 6. This is very interesting because it improves the smoothing results.

Another evaluation is done with the bearing 4 of testing 1 run-to-failure acceleration vibration signals ending with a roller element defect. Fig. 25 shows the bearing 4 of testing 1 run-to-failure acceleration vibration signals. Fig. 26–28 show respectively the RMS, the Kurtosis and the RMSEE measurement of the tested bearing. Experimental results given in Figs. 29 and 30 illustrate that the proposed method can reliably predict the RUL of rolling element bearings based on the SFAM neural network.

As conclusion, the proposed SFAM online approach is able to follow the degradation of the two tested REBs despite that they have neither the same life nor the same type of failure compared to the bearing used in the offline training phase. The evaluation of the proposed method shows that it is a good technique and a sound methodology for REB fault prognosis.

5. Discussion and comparison with some previous works

This section presents a comparison of the proposed method by specifying the advantages of its fits compared to previous works. Table 7 summarizes some previous works based on physical model and data-driven model for REB prognostics.

In literature, the most used approaches are those based on physical models and data-driven approaches. Physical models require the estimation of various physics parameters. Data-driven approaches, including simple projection models, are advantaged by the simplicity of their calculations, which can be carried out on a programmable calculator [2]. The work

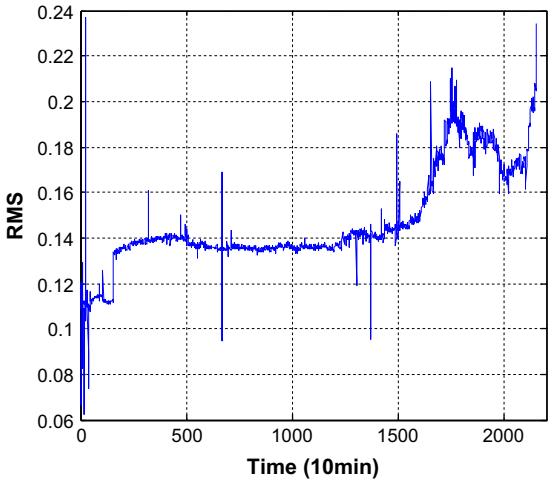

Fig. 26. RMS of the bearing 4 of testing 1.

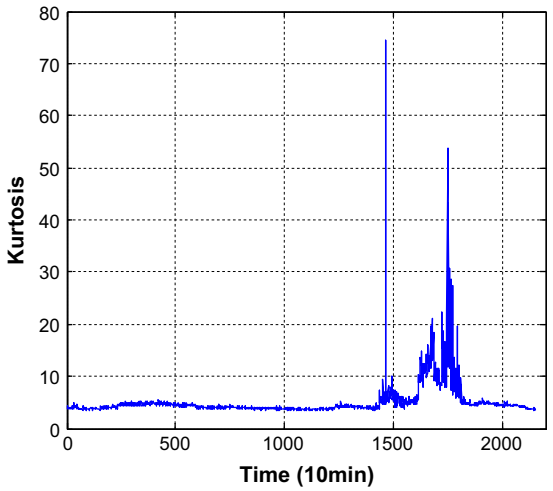

Fig. 27. Kurtosis of the bearing 4 of testing 1.

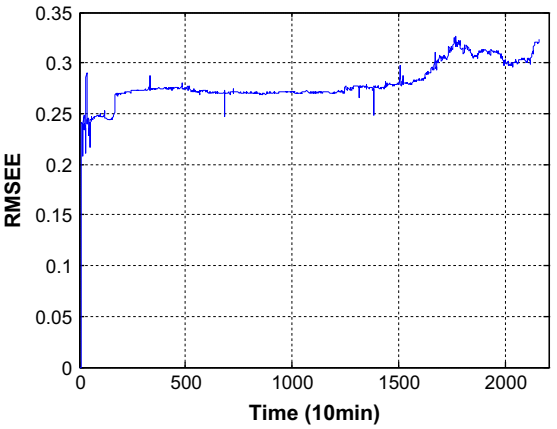

Fig. 28. RMSEE of the bearing 4 of testing 1.

presented in this paper is based on data-driven approaches. The novelty of this work is that it transforms the prognostic task into a simple classification task. This general method can be applied and for the prognostics of a wide variety of industrial assets. Besides, it requires a single monitoring history for the training regardless of type and nature of the failure. Moreover,

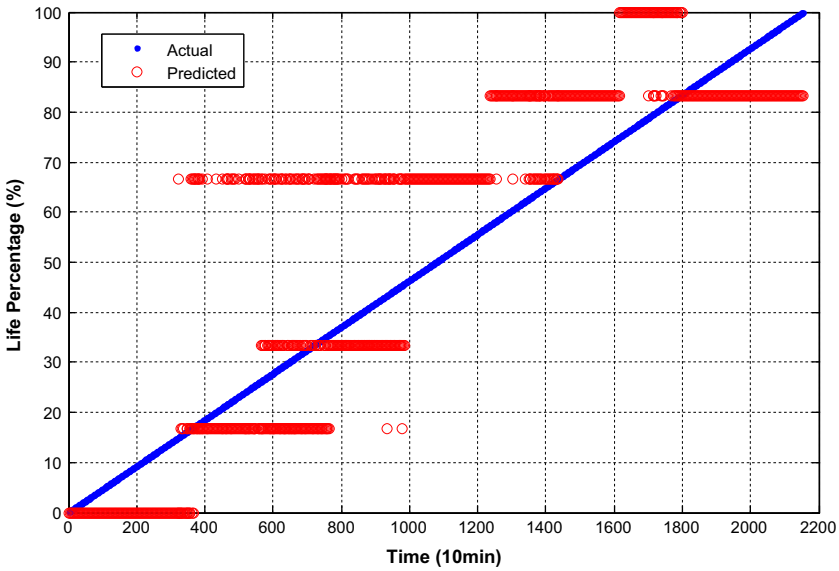

Fig. 29. Online classification of bearing rate failure (bearing 4 of testing 1).

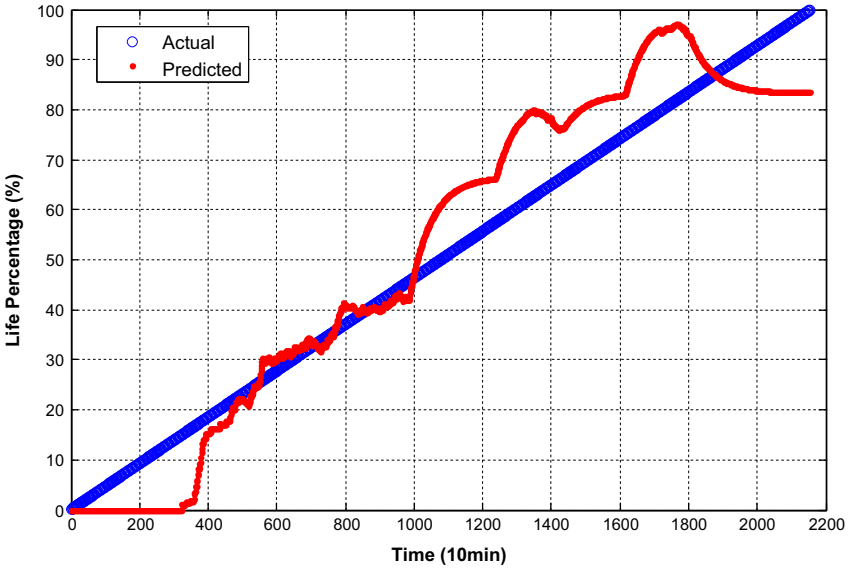

Fig. 30. RUL prediction of the bearing 4 of testing 1 test failure history.

it does not require a priori knowledge of the tested assets; it needs just a one failure history in the training phase. The proposed methodology exhibits good ability of forecasting degradation assets to reduce maintenance costs. As conclusion, the evaluation of the proposed method versus those in previous researches, given in Table 7, shows that the proposed approach is a sound methodology. It is less complex in terms of calculation and it is very adequate to estimate the future health of monitored assets. The prediction of bearing RUL based on SFAM neural network has not been applied before this research. This work will significantly accelerate the advancement of prognostic researches.

Finally, it is stated that more than 50% of the failures are mechanical in nature, such as bearing, mechanical faults in rotors, imbalance, and alignment-related problems [33]. The prediction of the RUL of bearings is still a great and a vast challenge for scientific and industrial researchers. As perspective, we will consider the filtering of the raw vibration signals and the separation of the multivariate vibration signals into additive subcomponents before extracting features. These considerations can generalize the robustness of the proposed methodology. We recall that in an industrial environment, signals that indicate bearing faults should be extracted from the overall vibration signals in normal machines with other background masking signals such as from rotating shafts, gears, pump vanes, etc.

Table 7
Comparison of this work with some previous researches.

Literature	Methodology	Advantages	Drawbacks
[19]	Data interpolation using Self-Organizing Map (SOM) and Back Propagation Neural Network (BPNN)	– Longer prediction horizon	– Requires training one BPNN for each historical dataset
[34]	Exponential projection using BPNN	– Longer prediction horizon instead of condition index at future time steps	– Requires training one BPNN for each historical dataset and assumes that all bearing degradation follow an exponential model
[8]	Bernstein distribution	– Do not require condition monitoring	– Traditional reliability model that requires huge computing and can be used only for the same bearing type
[35]	Proportional Hazards Models and transition probability	– Trends data features characterization and considers economical conditions	– The use of a large condition monitoring histories
[16]	ISOMAP and SVR	– Requires a single condition monitoring history for the training	– Does not provide a good indication of time and probability failure
Proposed methodology	SFAM and Weibull distribution	– Requires a single condition monitoring history for the training. – Can be applied using different classifiers – Do not require a priori knowledge of the tested assets – Longer prediction horizon	– Do not consider variable operating conditions – Does not detect the type of fault

6. Conclusion and future works

Accurate bearing RUL prediction is critical to effective condition based maintenance for improving reliability and reducing overall maintenance cost. In this work, an effort is made to characterize and classify seven different REB classes depending on their vibration features. An intelligent method is proposed for achieving more accurate bearing RUL prediction based on SFAM neural network. Besides, a new feature that better follow REB degradation is proposed. To validate the proposed method, the condition monitoring data collected from bearings are used. Experiment results show that the proposed method can produce satisfactory RUL prediction results. Also, experimental results demonstrate the ability of the proposed combination of SFAM and Weibull distribution for REB failure prognostics. Indeed, variable operating conditions (speed and torque) and the suitability method to noises and background masking signals are the aspects of the ongoing works which may help generalizing the proposed method.

Acknowledgement

The authors would like to thank the center on Intelligent Maintenance Systems (IMS) University of Cincinnati, USA, for providing the bearing dataset. Also, authors would like to thank Dr Barrie William Jervis (former professor in Sheffield Hallam University (U.K)) for his relevant advices during the implementation of the SFAM neural network.

Appendices

A. SFAM training process

When an input vector is presented to the network, it is first preprocessed into complement coded form. The resulting vector is called I. The activity pattern on layer F_1 is set equal to I. The choice function is then evaluated for each neuron of F_2. Mathematically, the choice function is defined by:

$$T_j = \frac{\left|I\hat{W}_j\right|}{\alpha + |W_j|}, \tag{A1}$$

where $|\ .\ |$ is the Euclidian norm, $\hat{}$ is the fuzzy "AND" operator and α is an arbitrary parameter greater than zero which is usually chosen close to zero for a good performance.

Once the winning neuron is selected, a vigilance criterion is evaluated. The vigilance criterion causes the network to choose another neuron if the first selected one is inadequate. Consequently, the vigilance parameter ρ is used to control the SFAM operations.

Mathematically, the vigilance criterion is governed by:

$$\frac{\left|I\hat{W}_j\right|}{|I|} \geq \rho, \tag{A2}$$

where j is the index of the evaluated neuron in F_2 and ρ is the vigilance parameter, which lies in the interval [0 1].

If the criterion is respected, the SFAM learns the input vector. Contrarily, it selects the next neuron with the uppermost choice function and re-evaluates the vigilance criterion.

These steps are repeated until the vigilance criterion is satisfied. It is then said that the network is in resonance: All F_2 components are set to 0 except the winning neuron which is set to 1.

In the resonance phase, the SFAM proceeds with the input vector I by modifying the weights W_G as follows:

$$W_G^{new} = \beta(I\hat{W}_G^{old}) + (1-\beta)W_G^{old}, \tag{A3}$$

where G is the index of the winning neuron and β is the learning rate ($\beta=1$ is used for fast learning mode).

Finally, the Y vector will be sent to the decision map through the W^{ab} connection to save the class which is already given by the input vector I. The different steps of the SFAM algorithm are given in appendix B. More details are given in [36–38].

B. SFAM algorithm

1. Training mode:
   Initialization:
   - All the neurons of F_2 are not made.
   - All the weights in W are set to 1.
   - All the weights in W^{ab} are set to 0.
2. Encoding of the input vector:
   - Present a vector, a, to the F_0 layer:

$$a = \{a_j \in [0\ 1]: i = 1,\ 2\ldots L'\} \tag{B1}$$

   - Coding in complement:

$$I = (a,\ a_c);\ a_c = 1 - a \tag{B2}$$

   - The vector I activates the F_1 layer.
3. Choice of category:
   - The choice function is calculated for each F_2 layer's neuron as:

$$T_j = \frac{\left|I\hat{W}_j\right|}{\alpha + |W_j|} \tag{B3}$$

   - F_2 is a competitive layer where the wining is the neuron G such as:

$$G = argmax\{T_j : j = 1,\ 2\ldots N\} \tag{B4}$$

4. The vigilance criterion:
   - Compare the similarity between I and W_G on the layer F_1 according to:

$$\frac{|I\hat{W}_G|}{|I|} = \frac{|I\hat{W}_G|}{M} \geq \rho \tag{B5}$$

   - Pass the test: Neuron G is selected and W_G can learn the input I (go to the step 5).
   - Fail the test: Inhibit the neuron G ($T_G = -1$) and return to step 5 to look for another neuron which can pass the test.
5. Prediction of a class:
   - The code of desired class t is transmitted to F^{ab}.

- Prediction function: The vector Y activates the F^{ab} layer via the W^{ab} weights:

$$S_G^{ab}(Y) = \sum_{j=1}^{N} (Y_j W_{jG}^{ab}) \tag{B6}$$

- Prediction:

$$K = argmax\ \{S_i^{ab}(Y): i = 1, 2 \ldots L\} \tag{B7}$$

- Active for the neuron K corresponding to the prediction ($Y_K^{ab} = 1$ and $Y_i^{ab} = 0$ if $i \neq K$);
- If the prediction K corresponds to the desired class t, go to step 6. Unlike, apply the "match tracking".
- Match tracking: increase ρ just enough as:

$$\rho = \rho + \varepsilon \tag{B8}$$

- To find another neuron made of F_2 which predicts the desired class t;
- To create a new neuron not-clerk of F_2 to learn the desired class if all neurons are tested.

6. Learning:
   - Update of the prototype G:

$$W_G^{new} = \beta(I\hat{W}_G^{old}) + (1-\beta)W_G^{old} \tag{B9}$$

   - Create a new associative neuron A if all neurons are inhibited ($W_{At}^{ab} = 1$ where t is the desired class).

Test mode:

- Step 2;
- Step 3;
- Step 5 (just prediction function and prediction sub-steps);
- Return to step 2 to take another test

Fig. B.1 shows the different steps of the SFAM algorithm.

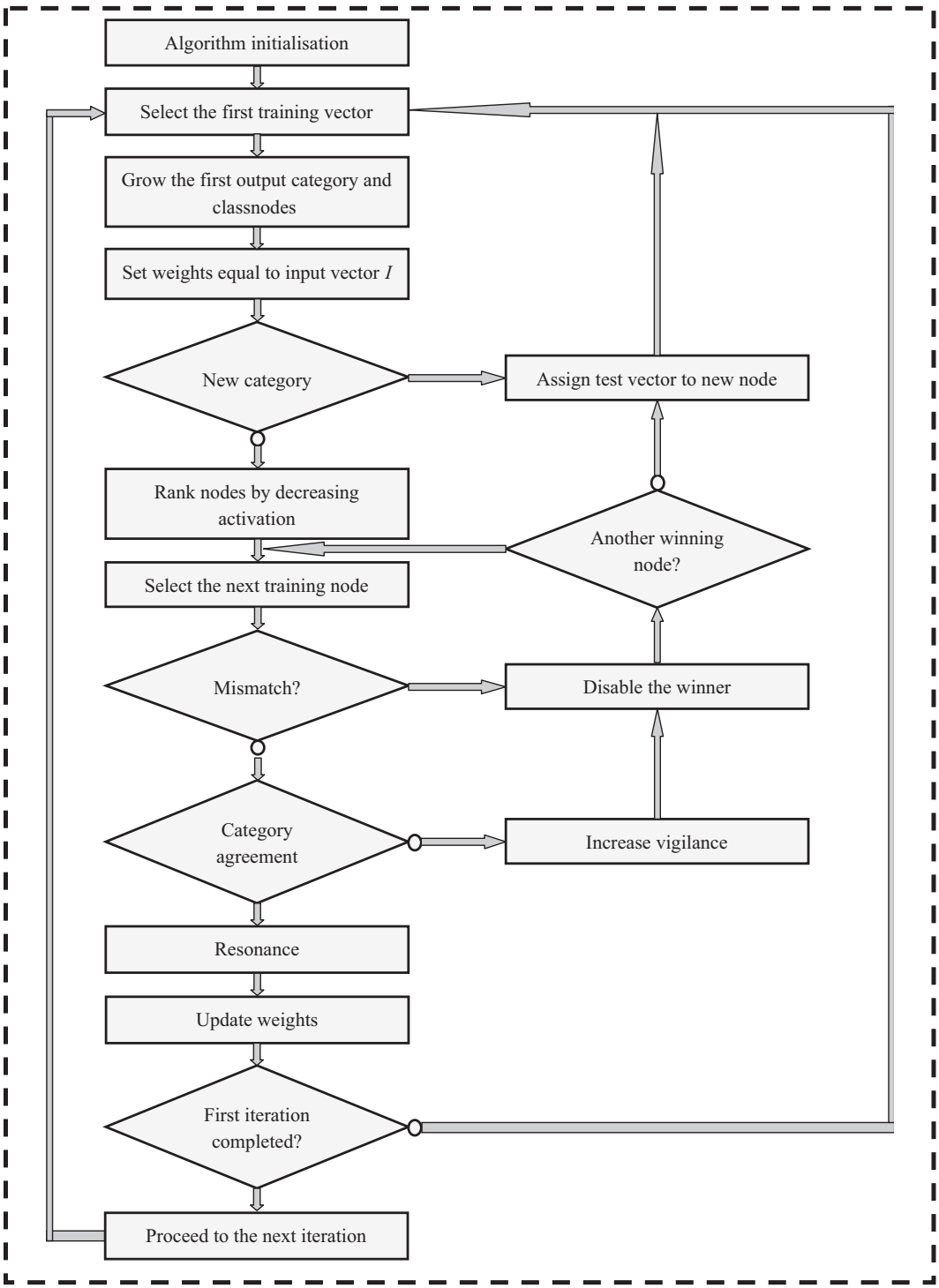

Fig. B.1. SFAM flowchart.

References

[1] D.A. Tobon-Mejia, K. Medjaher, N. Zerhouni, The ISO13381-1 standard's failure prognostics process through an example,in: IEEE Prognostics & System Health Management Conference, University of Macau, Macau, China, 2010.
[2] A. Heng, S. Zhang, A.C.C. Tan, J. Mathew, Rotating machinery prognostics: state of the art, challenges and opportunities, Mech. Syst. Sig. Process. 23 (2009) 724–739.

[3] J. Ben Ali, N. Fnaiech, L. Saidi, B. Chebel-Morello, F. Fnaiech, Application of empirical mode decomposition and artificial neural network for automatic bearing fault diagnosis based on vibration signals, Appl. Acoust. 89 (2015) 16–27.
[4] J. Coble, W. Hines, Identifying optimal prognostic parameters from data:a genetic algorithms approach," in: Annual Conference of the Prognostics and Health Management Society, USA, 2009.
[5] T. Brotherton, G. Jahns, J. Jacobs, D. Wroblewski, Prognosis of fauls in gaz turbine engines, Intell. Aerosp. Conf. Proc. IEEE (2000) 163–171.
[6] S. Nandi, H.A. Toliyat, L. Xiaodong, Condition monitoring and fault diagnosis of electrical motors—a review, IEEE Trans. Energy Convers. 20 (2005) 719–729.
[7] J. Ben Ali, M. Sayadi, F. Fnaiech, B. Morello, N. Zerhouni, Importance of the fourth and fifth intrinsic mode functions for bearing fault diagnosis," in: 14th International Conference on Sciences and Techniques of Automatic Control and Computer Engineering (STA), 259-264, 2013.
[8] G. Nagi, E. Alaa, P. Jing, Residual Life predictions in the absence of prior degradation knowledge, IEEE Trans. Reliab. 58 (2009) 106–116.
[9] S. Sadok, B. Bechir, T. Marc, A numerical model to predict damaged bearing vibrations, J. Vib. Control 13 (2007) 1603–1628.
[10] L. Saidi, J. Ben Ali, F. Fnaiech, Bi-spectrum based-EMD applied to the non-stationary vibration signals for bearing faults diagnosis, ISA Trans. 53 (2014) 1650–1660.
[11] A. Widodo, B-S. Yang, Support vector machine in machine condition monitoring and fault diagnosis, Mech. Syst. Sig. Process. 21 (2007) 2560–2574.
[12] R.B. Randall, J. Antoni, Rolling element bearing diagnostic—a review, Mech. Syst. Sig. Process. 25 (2011) 485–520.
[13] F. Olga, Z. Enrico, W. Ulrich, Predicting component reliability and level of degradation with complex-valued neural networks, Reliab. Eng. Syst. Saf. 121 (2014) 198–206.
[14] A.K. Mahamad, S. Saon, T. Hiyama, Predicting remaining useful life of rotating machinery based artificial neural network, Comput. Math. Appl. 60 (2010) 1078–1087.
[15] T. Zhigang, An artificial neural network method for remaining useful life prediction of equipment subject to condition monitoring, J. Intell. Manuf. 23 (2012) 227–237.
[16] T. Benkedjouh, K. Medjaher, N. Zerhouni, S. Rechak, Remaining useful life estimation based on nonlinear feature reduction and support vector regression, Eng. Appl. Artif. Intell. 26 (2013) 1751–1760.
[17] A. Malhi, R.X. Gao, PCA-based feature selection scheme for machine defect classification, IEEE Trans. Instrum. Meas. 6 (2004) 1517–1525.
[18] W. Kuo, M.J. Zuo, Optimal Reliability Modeling: Principles and Applications, Wiley, Hoboken, 2003.
[19] H. Runqing, X. Lifeng, L. Xinglin, L.C. Richard, Q. Hai, L. Jay, Residual life predictions for ball bearings based on self-organizing map and back propagation neural network methods, Mech. Syst. Sig. Process. 21 (2007) 193–207.
[20] N. Tandon, A. Choudhury, A review of vibration and acoustic measurement methods for the detection of defects in rolling element bearings, Tribol. Int. 32 (1999) 469–480.
[21] P. Nectoux, R. Gouriveau, K. Medjaher, E. Ramasso, B. Morello, N. Zerhouni, C. Varnier, "PRONOSTIA: an experimental platform for bearings accelerated degradation tests, in: IEEE International Conference on Prognostics and Health Management, PHM'12, Denver, Colorado: United States, 2012.
[22] H.Y. Yang, M. Joseph, L. Ma, Fault diagnosis of rolling element bearings using basis pursuit, Mech. Syst. Sig. Process. 19 (2005) 341–356.
[23] P. Tao, J. Haiyan, X. Yong, "Weibull distribution parameters for fault feature extraction of rolling bearing, in: Chinese Control and Decision Conference (CCDC), IEEE, China, 2011, pp. 69–74.
[24] A. Nasr, S. Gasmi, M. Sayadi, Estimation of the parameters for a complex repairable system with preventive and corrective maintenance, in: IEEE Proc, International Conference on Electrical Engineering and Software Applications (ICEESA), Tunisia, 2013, pp. 1–6.
[25] A.A. Nasir, M.Y. Mashor, R. Hassan, Classification of Acute Leukaemia Cells using Multilayer Perceptron and Simplified Fuzzy ARTMAP Neural Networks, Int. Arab J. Inf. Technol. 10 (2013) 356–364.
[26] G.A. Carpenter, S. Grossberg, Pattern Recognition by Self-Organizing Neural Networks, MIT Press, Cambridge, MA, 1991.
[27] P. Venkatesan, M. Suresh, Classification of Renal Failure Using Simplified Fuzzy Adaptive Resonance Theory Map, Int. J. Comput. Sci. Network Secur. 9 (2009) 129–134.
[28] S. Rajasekaran, G. Pai, Image Recognition Using Simplified Fuzzy ARTMAP Augmented with a Moment Based Feature Extractor, Int. J. Pattern Recogn. Artif. Intell. 14 (2000) 1081–1095.
[29] IMS bearings data set (2014) "⟨http://ti.arc.nasa.gov/tech/dash/pcoe/prognostic-data-repository/⟩".
[30] H. Qiu, J. Lee, J. Lin, G. Yu, Robust performance degradation assessment methods for enhanced rolling element bearing prognostics, Adv. Eng. Inf. 17 (2003) 127–140.
[31] H. Qiu, J. Lee, J. Lin, G. Yu, Wavelet filter-based weak signature detection method and its application on rolling element bearing prognostics, J. Sound Vib. 289 (2006) 1066–1090.
[32] T. Zhigang, W. Lorna, S. Nima, A neural network approach for remaining useful life prediction utilizing both failure and suspension histories, Mech. Syst. Sig. Process. 24 (2010) 1542–1555.
[33] Ş. Tayfun, K. Erinç, Ş. Serhat, A new MLP approach for the detection of the incipient bearing damage, Adv. Electr. Comput.Eng. 10 (2010) 34–39.
[34] N. Gebraeel, M. Lawley, R. Liu, V. Parmeshwaran, Residual life predictions from vibration-based degradation signals: a neural network approach, IEEE Trans. Ind. Electron. 51 (2004) 694–700.
[35] D. Banjevic, A.K.S. Jardine, Calculation of reliability function and remaining useful life for a Markov failure time process, IMA J. Manage. Math. 17 (2006) 115–130.
[36] B.W. Jervis, S. Djebali, L. Smaglo, Integrated probabilistic simplified fuzzy ARTMAP, IEE Proc.: Sci. Meas. Technol. 151 (2004) 218–228.
[37] B.W. Jervis, T. Garcia, E.P. Giahnakis, The probabilistic simplified Fuzzy ARTMAP (PSFAM), IEEE Proc. Sci. Meas. Technol. 146 (1999) 165–169.
[38] J. Ben Ali, S. Abid, B.W. Jervis, F. Fnaiech, C. Bigan, M. Besleaga, Identification of early stage Alzheimer's disease using SFAM neural network, Neurocomputing 143 (2014) 170–181.